Direct Numerical Simulation of Laminar and Turbulent Rayleigh-Bénard Convection

Firas Dabbagh

Abstract

The main aim of this work is understanding the phenomenon of Bénard cells in laminar and turbulent regimes as an application of studying the air flow in the air gap and honey comb cells that installed in the flat plate solar collector. Furthermore analyzing the turbulent Rayleigh-Bénard convection components by performing direct numerical simulation of turbulent air flow in too long inclined cavity like the air gap. The first two parts treat with known problems of laminar and turbulent flow as a necessary presentation of numerical methods used in solving the governing equation of flow motion and heat transfer, afterward the third part deals with the main object of investigating the turbulent and laminar Rayleigh-Bénard convection flow.

1 Driven cavity and backward-facing step problems

The well-known driven cavity and backward-facing step problems have been treated in 2-D view where finite volume discretization method (FVM) has been utilized and the governing momentum Navier-Stokes equations in non-dimensional form have been resolved on structured and staggered grids. A fully explicit second-order Adams-Bashforth scheme is used and the fractional step projection method that is derived from the well-known Helmholtz-Hodge vector decomposition theorem, has been used as an explicit algorithm for decoupling the pressure and velocity fields. The solutions are bounded by driven horizontal forced flow at the top and no-slip boundaries at the rest walls in the square driven cavity problem, while they bounded by a fully developed horizontal velocity profile yields to unity mean value at the inlet and Nuemann conditions at the outlet with no-slip boundary conditions at the step,roof and the floor of the channel, Quick numerical scheme has been used in evaluating the convective term in the momentum equations. Comparisons with the Benchmark results [11] of velocity profiles have done in the case of driven cavity problem (see figure 1), and with the measured results taken from 3-D experiments of Armaly et al. [1] at the symmetric plane where the span width is $35h$ (see figure 2), it is found a good agreements to validate the code used.

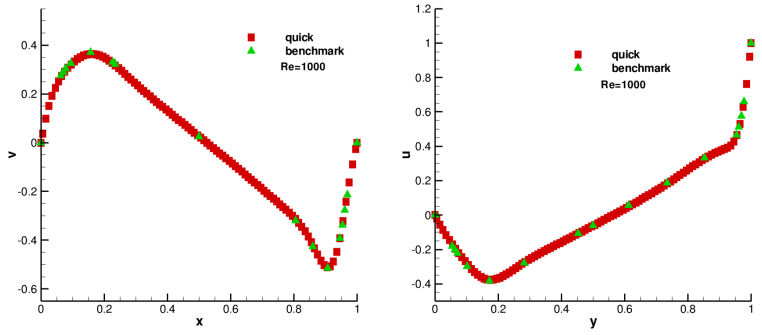

(a) v at mesh 100x100 (b) u at mesh 100x100

Figure 1: Values of v(a) and u(b) along the horizontal and vertical middle line of the cavity respectively, at $Re = 1000$.

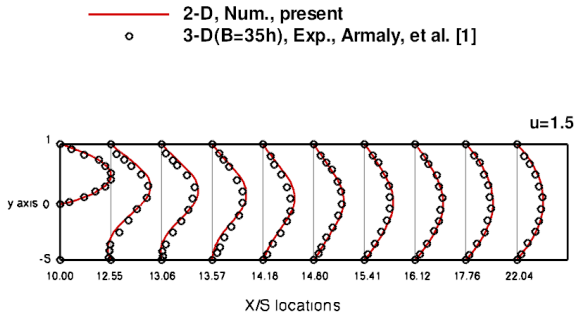

Figure 2: Streamwise velocity profiles at the $z = 0$ symmetric plane for the case $Re = 100$.

2 Direct numerical simulation of Turbulent and laminar air flow in differentially heated cavity

The laminar and turbulent air flow in a differentially heated cavity of aspect ratio 1 and 4, are treated in 2-D view where the non-dimensional momentum and energy equations have been solved employing FVM discretization on structured and staggered grids. As known, the studied problem reflects the air motion induced by the buoyancy forces that are a result of heating the vertical opposite walls differentially, the horizontal walls are adiabatic with implying no-slip boundary conditions at all the walls. Second order and fourth order symmetry-preserving schemes are applicate in evaluate the linear and nonlinear terms of Navier-Stokes equations, they are reported by R.W.C.P. Verstappen and A.E.P. Veldman [2], these scheme conserve the kinetic energy without systematically to be damped by discrete convective operator, The one-leg second-order-explicit time integration scheme (k**1**L**2**) with the Eigen**CD** method proposed by

F.X.Trias and O.Lehmkuhl [3] have been used to maximize the time step without losing the accuracy of the solution. Comparisons against the Benchmark results reported by G. de Vahl Davis [4] in the square cavity and X. Trias [4] and S. Xin [5] results have done and found so good agreement with those presented.

	$Ra = 10^3$		$Ra = 10^4$		$Ra = 10^5$		$Ra = 10^6$	
	$error_1$%	$error_2$%	$error_1$%	$error_2$%	$error_1$%	$error_2$%	$error_1$%	$error_2$%
Nu_{max}	0.194%	0.066%	0.529%	0.17%	2.4%	0.35%	5.21%	0.44%
y	1.9%	6.52%	0.524%	0.7%	0.3%	5.3%	7.4%	6.58%
Nu_{min}	0.159%	0.144%	0.2%	0.001%	0.2%	0.001%	0.78%	0.78%
y	0.625%	0.2%	0.625%	0.3%	0.625%	0.2%	0.5%	0.2%
Nu_{2D}	0.11%	0.001%	0.516%	0.313%	1.1%	0.377%	2%	0.47%
v_{max}	0.008%	0.189%	0.04%	0.3%	0.001%	0.087%	0.69%	0.468%
x	1.82%	1.685%	0.21%	5%	4.16%	4.54%	7.65%	6.58%
u_{max}	0.044%	0.246%	0.013%	0.068%	0.293%	0.31%	0.9%	0.6%
y	0.7%	0.861%	0.516%	0.243%	0.146%	0.35%	0.58%	1%

Table 1: Summery of percentage of deviation from the Benchmark results,($error_1$) uniform grid, ($error_2$) grid with refinement.

Ra	$6.4\text{x}10^8$	$2\text{x}10^9$	10^{10}
$\overline{Nu}$	49.23	66.22	100.60
$\overline{Nu}_{XQ}$	49.2	66.5	101.0
Nu_{max}	169.88	248.80	446.30
y	$4.50\text{x}10^{-3}$	$2.60\text{x}10^{-3}$	$8.45\text{x}10^{-4}$
Nu_{min}	2.58	3.41	5.16
y	1	1	1
$< u >_{max}$	$2.33\text{x}10^{-2}$	$2.01\text{x}10^{-2}$	$8.45\text{x}10^{-3}$
y	$9.49\text{x}10^{-1}$	$9.48\text{x}10^{-1}$	$9.58\text{x}10^{-1}$
$< v >_{max}$	$2.23\text{x}10^{-1}$	$2.23\text{x}10^{-1}$	$2.29\text{x}10^{-1}$
x	$7.50\text{x}10^{-3}$	$5.79\text{x}10^{-3}$	$3.90\text{x}10^{-3}$

Table 2: Summery of the averaged flow feature results where $\overline{Nu}_{XQ}$ is the averaged Nusselt number presented by [5].

Later an improvement of the code to solve three dimensional cases and simulate a turbulent Rayleigh-Bénard convection in a cavity of aspect ratio 0.5 has done with validation of the code against Benchmark results. However, the limits of using just one CPU prevented using smoother grids and the parallelization was the solution. A simple parallel code has performed to solve huge linear system equations by more than one CPU, applying the MPI parallel mode.

3 Direct numerical simulation of Turbulent and laminar Rayleigh Bénard convection

Understanding the phenomena of Bénard cells in laminar and turbulent views and its widely appearance in many engineering applications like the solar collector, was the main aim of this work. A parallel special code developed by the center (Heat and Mass transfer tecnological center) has been used to perform three dimensional numerical simulation of the air flow in inclined cavity by $\theta = 40^\circ$ heated from below and cooled from above at $Ra = 2.47\text{x}10^5$, at different values of the aspect ratio $\Gamma_1 = L/H$(ratio in length direction respect to the height of cavity) and $\Gamma_2 = W/H$(ratio in the spanwise direction also respect to the height). It represents a direct simulation for improving the design of the plastic honey comb cells that installed in the flat plate solar collectors where high thermal resistance material can be used and installed in relatively small volume.
A Primarily two-dimensional study has done to see the influence of the aspect ratio on the Nusselt number. They showed that the Nu_{2D} increases rapidly when Γ_1 changes from 0.1875 to 0.25 since the air goes from a throttle state to more free one. No influence of initial temperature was found in these outlines but its noted in the 3-D simulation, its effect is limited in changing the rotation direction when the flow becomes three dimensional in the adiabatic side boundaries case. Bénard cells are evolved along the horizontal periodic spanwise direction at particular distance and repeated at relative larger ones until become stable. To express the infinite general spanwise distance that can be represented by set the periodic side boundaries, its found that the minimum span width should be enough to formulate two completed rolls suited to Γ_1, which leads to permanent and not changed Nusselt number with increasing the periodic cut distance. This span width is detected to be of aspect ratio $\Gamma_2 > 1$ when $\Gamma_1 = 0.25$ and $Ra = 2.47\text{x}10^5$. Two arrangement design of the plastic cells have been proposed, in designing the small cells (adiabatic side boundaries) or the infinite parallel rows (periodic side boundaries), they were detected to be $\Gamma_1 = \Gamma_2 = 0.1875$ in case of small closed cells and $\Gamma_1 = 0.0625$ in the case of parallel rows. However, they have been found so costly and placing a plastic plate horizontally in the air gap which can divides the flow can be a future work in damping the air motion and reduce the heat losses by convection.

Afterward at very large aspect ratio $\Gamma_1 = 50$, the flow has been evolved to turbulent form. Thermal mushroom-like plumes of large-scale relatively similar to those appeared in the cases of turbulent Rayleigh-Bénard convection in no titled convective cell, have been detected in the center area and coherent circulations are clustered near the side walls. Temporal study have been performed to investigate the Gaussianity of the flow in different part of turbulent domain by finding the histogram, skewness and kurtosis of the temperature at different heights between the isothermal walls. Its found high deviation from Gaussianity at the boundary layers and reduced gradually in the bulk to become zero at the center where a smaller correlation between the turbulent fields of temperature and velocity is detected comparing with the boundary layer areas. High amplitudes and inttermitency of the thermal dissipation rate that considered as a main important parameter in Turbulent Rayleigh-Bénard heat transport con-

vection, were found near the isothermal walls and the thermal plume regions, where the PDF statistics of ε_T were found to be tail stretched exponential distribution, and the tail becomes fatter in the boundary layers compared with the bulk, its found that it is following the passive scalar behavior in the bulk region and presents high intermittent magnitudes reflecting the small-scale intermittency that has its importance in DNS turbulent studies.
A partitioning of the domain was presented according the PDF of the normalized thermal dissipation rate(see figure 5), to (1) Gaussian or turbulent background region (so small values of thermal dissipation rate distributed in the bulk (mixing zones) and side wall areas) (2) thermal plumes region (high relatively values of thermal dissipation rate distributed in the boundary layer and the bulk where the plumes arose (ridges) and propagated (caps))(3) conductive sublayer region (very high values of thermal dissipation rate located in the boundary layers so close to the isothermal walls in the areas of interactions between the arising roots and descending caps of thermal plumes).
A study of mesh density and adequacy of the periodic side distance have done by testing the Grötbach criterion [10] that estimates the Kolmogorov dissipation scale and evaluating the two-points correlation to verify the satisfactory of the periodic distance, its found that $\Gamma_2 = 4$ is sufficient and the used mesh is enough to resolve the smallest relevant turbulent scales where the one-dimensional energy spectra in the periodic direction at a center point was performed and detected the Kolmogorov law $-5/3$ in velocity energy spectra and Bolgiano exponent $-7/5$ in the temperature one but its so difficult to distinguish. All these observations correspond very well with the events of turbulent Rayleigh-Bénard convection that found in literature like M. Emran & J. Schumacher [6], M. Kaczorowski & C. Wagner [7] and O. Shishkina & C. Wagner [8].

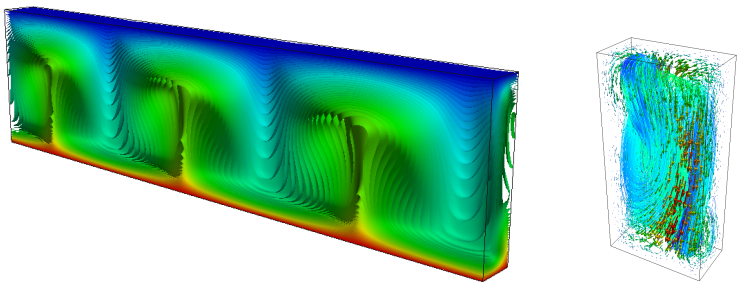

(a) (b)

Figure 3: (a)Isothermal planes at configurations $\Gamma_1 = 0.25$ and $\Gamma_2 = 4$ (periodic side boundaries), (b) Stream lines at Streamlines at configurations $\Gamma_1 = 0.25$ and $\Gamma_2 = 0.5$ (adiabatic side boundaries).

Studying cases with higher Rayleigh number at this configuration can be a so efficient future advancing work in investigating the turbulent Rayleigh-Bénard convection that have many applications in solar energy field.

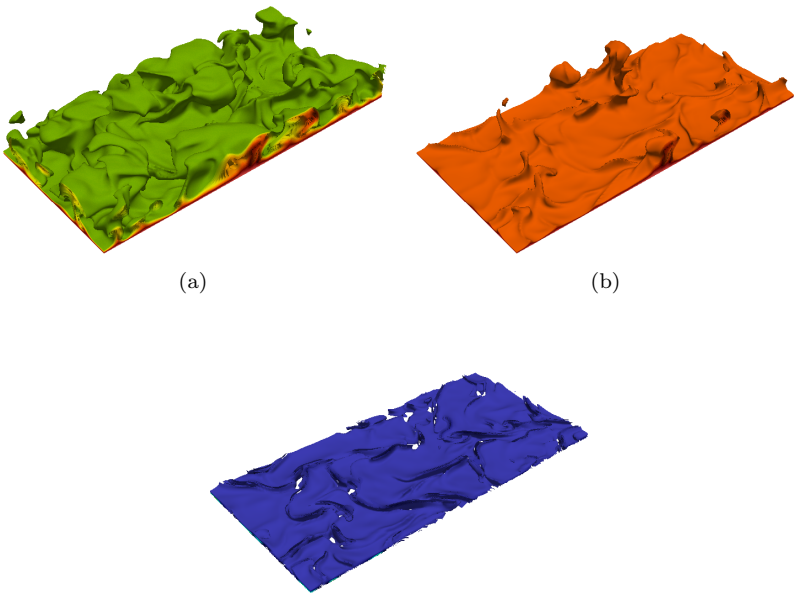

(a) (b)

(c)

Figure 4: Extracted instantaneous zoomed section of the hot thermal plumes at temperature range $0.5 \rightarrow 1$ (a), their stems $0.8 \rightarrow 1$ (b) and the corresponding thermal dissipation rate ε_T through a clip of height $0.3H$ (c).

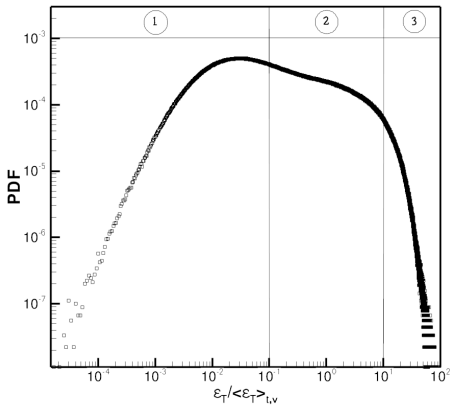

Figure 5: PDF of the normalized thermal dissipation rate $\varepsilon_T / < \varepsilon_T >_{t,v}$ in $log - log$ scales, the data are taken of gathering a sequence of independent snapshots.

References

[1] B. F. Armaly, F. Durst, J. C. F. Pereira, and B. Schönung, "Experimental and theoretical investigation of backward-facing step flow ", *J. Fluid Mesh*,

127, 473, 1983.

[2] R.W.C.P. Verstappen , A.E.P. Veldman, "Symmetry-preserving discretization of turbulent flow ", *J. Comput. Phys.*, vol. 187, pp. $343 - 368, 2003$.

[3] F. X. Trias and O. Lehmkuhl, "A self-adaptive strategy for the time integration of Navier-Stokes equations ", Taylor & Francis Group, LLC (2011).

[4] F. X. Trias, M. Soria, A. Oliva, and C. D. Pérez-Segarra, "Direct numerical simulations of two- and three-dimensional turbulent natural convection flows in a differentially heated cavity of aspect ratio 4 ",*Journal of Fluid Mechanics*, submitted 2006.

[5] S. Xin and P. Le Quéré, "Direct numerical simulation of two-dimensional chaotic natural convection in a differentially heated cavity of aspect ratio 4 ", *Journal of Fluid Mechanics*, **304** : $87 - 118$, 1995.

[6] G. de Vahl Davis and I. P. Jones, "Natural convection in a square cavity: a comparison exercise ", *International Journal for Numerical Methods in Fluids*, **3** : $227 - 248, 1983$.

[7] M. S. Emran & J. Schumacher 2012 "Conditional statistics of thermal dissipation rate in turbulent Rayleigh-Bénard convection ", *Eur. Phys. J.*,**35** 108.

[8] M. Kaczorowski & C. Wagner "Analysis of the thermal plumes in turbulent Rayleigh-Bénard convection based on well-resolved numerical simulations ", *J. Fluid Mech.* vol.**618** $89 - 112$, 2009.

[9] O. Shishkina & C. Wagner "Analysis of thermal dissipation rates in turbulent Rayleigh-Bénard convection ", *J. Fluid Mech.* vol.**546** $51 - 60$, 2006.

[10] G. Grötzbach. "Spatial resolution requirements for direct numerical simulation of the Rayleigh-Bénard convection ", *Journal of computational physics*, **49**:$241 - 264$,1983.

[11] Guia, U., Ghia, K. and Shin, C., 1982. "High-Re solutions for incompressible flow using the Navier Stokes equations and a multigrid method ", *J. Comput. Phys.*, **48**, $387 - 411$.